cmgh
CELLULAR AND MOLECULAR GASTROENTEROLOGY AND HEPATOLOGY

ORIGINAL RESEARCH

# Necroptosis Is an Important Severity Determinant and Potential Therapeutic Target in Experimental Severe Pancreatitis

Johanna M. Louhimo,[1] Michael L. Steer,[2] and George Perides[2]

[1]Department of Surgery, University of Helsinki, Helsinki, Finland; [2]Department of Surgery, Tufts Medical Center, Tufts University School of Medicine, Boston, Massachusetts

**SUMMARY**

During experimental acute pancreatitis, pancreatic acinar cells die primarily because of necroptosis. Inhibition of necroptosis either by administration of necrostatin or by genetic manipulation ameliorates the severity of acute pancreatitis. Delayed pharmacologic inhibition of necroptosis also reduces disease severity.

**BACKGROUND & AIMS:** Severe acute pancreatitis is characterized by acinar cell death and inflammation. Necroptosis is an aggressive and proinflammatory mode of cell death that can be prevented by necrostatin-1 administration or receptor-interacting protein kinase (RIP3) deletion.

**METHODS:** Mouse pancreatic acinar cells were incubated with supramaximally stimulating concentrations of caerulein or submicellar concentrations of taurolithocholic acid-3-sulfate (TLCS), and necroptosis was inhibited by either addition of necrostatin or by RIP3 deletion. Cell death was quantitated using either lactate dehydrogenase leakage from acini or propidium iodide staining of nuclei. Necrosome formation was tracked and quantitated using cell fractionation or immunoprecipitation. Pancreatitis was induced in mice by retrograde intraductal infusion of TLCS or by repetitive supramaximal stimulation with caerulein.

**RESULTS:** Necroptosis was found to be the most prevalent mode of acinar cell in vitro death and little or no apoptosis was observed. Acinar cell death was associated with necrosome formation and prevented by either necrostatin administration or RIP3 deletion. Both of these interventions reduced the severity of TLCS- or caerulein-induced pancreatitis. Delaying necrostatin administration until after pancreatitis already had been established did not prevent its ability to reduce the severity of TLCS-induced pancreatitis.

**CONCLUSIONS:** Necroptosis is the predominant mode of acinar cell death in severe experimental mouse pancreatitis. The severity of pancreatitis can be reduced by administration of necrostatin, and necrostatin still can reduce the cell injury of pancreatitis even if it is administered after the disease already has been established. Inhibition of necroptosis may be an effective strategy for the treatment of severe clinical pancreatitis. *(Cell Mol Gastroenterol Hepatol 2016;2:519–535; http://dx.doi.org/10.1016/j.jcmgh.2016.04.002)*

*Keywords:* Acute Pancreatitis; Biliary Pancreatitis; Necroptosis; Apoptosis; Pancreatic Cell Death.

Acute pancreatitis is a relatively common but poorly understood inflammatory disease involving the exocrine pancreas. To date, no specific treatment for acute pancreatitis has been identified. The majority of patients with mild acute pancreatitis recover quickly without specific treatment, but roughly 20% of patients with severe pancreatitis, most of whom have evidence of pancreatic necrosis, experience significant morbidity and a mortality rate that can approach 20%.[1,2] The mechanisms responsible for pancreatic necrosis in acute pancreatitis and the basis for the high mortality rate in the subgroup of patients with severe necrotizing pancreatitis are poorly understood, but a better understanding of these phenomena and identification of interventions that could reduce the severity of pancreatitis are likely to have considerable impact on the treatment and outcome of this relatively common disease.

Until recently, only 2 forms of cell death had been recognized: a regulated programmed form of cell death, referred to as *apoptosis*, and an unregulated or accidental form of cell death, loosely referred to as *necrosis*. Apoptosis can be mediated by either extrinsic or intrinsic mechanisms, and most apoptotic cell death involves caspase-dependent events. It is characterized morphologically by cell shrinkage and other characteristic cell changes in the absence of an inflammatory response. Terminal deoxynucleotidyl transferase–mediated deoxyuridine triphosphate nick-end labeling (TUNEL) staining and measurement of caspase activity are 2 of many methods of timing and quantitating the onset and extent of apoptosis. Apoptosis also is sensitive to inhibition by the pancaspase inhibitor benzyloxycarbonyl-Val-Ala-Asp (OMe) fluoromethylketone (Z-VAD-fmk) (reviewed by Galluzzi et al[3]).

***Abbreviations used in this paper:*** **AMC, 4-amido-methylcoumarin; ATP, adenosine triphosphate; BAPTA, 2-bis (2-aminophenoxy)-ethane-*N,N,N′,N′*-tetraacetic acid; DMEM, Dulbecco's modified Eagle medium; DMSO, dimethyl sulfoxide; IL, interleukin; LDH, lactate dehydrogenase; MCP-1, monocyte chemoattractant protein-1; MLKL, mixed-lineage kinase like; PI, propidium iodide; RIP, receptor-interacting protein kinase; TBS, Tris-buffered saline; TLCS, taurolithocholic acid-3-sulfate; TUNEL, terminal deoxynucleotidyl transferase–mediated deoxyuridine triphosphate nick-end labeling; Z-VAD-fmk, benzyloxycarbonyl-Val-Ala-Asp (OMe) fluoromethylketone; Z-DEVD, benzyloxycarbonyl-Asp-Glu-Val-Asp-aminomethylcoumarin.**

Most current article



2352-345X
http://dx.doi.org/10.1016/j.jcmgh.2016.04.002

In contrast to apoptosis, necrosis is characterized morphologically by a gain in cell volume, swelling of organelles, plasma membrane rupture, extravasation of intracellular contents, and the presence of an acute inflammatory response.[4] In the past, necrosis was thought to always be an accidental and uncontrollable mode of cell death, but recent observations have indicated that some forms of cell death that morphologically appear to be necrotic are, in fact, finely regulated by a set of intracellular signal transduction pathways.[5] The best-characterized and most widely studied of these regulated forms of necrosis is necroptosis.[3] Necroptosis has been observed to occur after ligation of death domain receptors (eg, binding of tumor necrosis factor-$\alpha$ to tumor necrosis factor–receptor 1) and the process of necroptosis is known to involve the activation and translocation of the receptor-interacting protein kinase (RIP)1 and RIP3 kinases and the pseudokinase mixed-lineage kinase like (MLKL) to a large, amyloid-like, multimolecular scaffold complex dubbed the *necrosome*.[6–9] By incompletely understood mechanisms, the assembled necrosome then can mediate necroptotic cell death. In some cases, necroptosis is thought to be autophagy-dependent,[10] however, by definition, it is always dependent on activation of the kinase RIP1[3,11] and it can be inhibited by either pharmacologic inhibition of RIP1 (eg, by small molecules known as necrostatins[12,13]) or by genetic deletion of RIP3.[1] Genetic deletion of RIP1 is embryonically lethal, but it now is known that activation of RIP1 depends on its association with RIP3 kinase[3,11] and, fortunately, genetic deletion of RIP3 is not embryonically lethal. As a consequence, prevention of RIP1 activation (followed by prevention of necrosome formation and necroptosis) can be accomplished experimentally by genetic deletion of RIP3. Recent data have shown that MLKL functions as the executioner molecule in necroptosis, targeting phosphatidylinositol binding sites and rupturing the plasma membrane.[14] The consequences of preventing necroptotic cell death appear to be cell- and disease state–specific. In some cases, it appears to promote alternative forms of cell death such as apoptosis, however, in other cases, prevention of necroptosis leads to events that favor cell survival.[13]

In the current article, we report the results of studies designed to examine the mode of pancreatic acinar cell death during the early stages of 2 experimental mouse models of severe pancreatitis: bile acid–induced and secretagogue-induced severe pancreatitis. Our studies had the following 4 primary goals: (1) to identify the most prevalent mode of cell death during the early stages of these 2 models of severe pancreatitis; (2) to examine the sequence and timing of some of the events related to acinar cell necroptotic cell death during the evolution of severe pancreatitis; (3) to define the effects on pancreatitis severity of inhibiting this most prevalent mode of cell death; and (4) to examine the possibility that inhibiting this mode of cell death can reduce the severity of pancreatitis even if that inhibition of cell death occurs after the start of pancreatitis induction.

# Materials and Methods

## Materials

The amylase substrate (2-chloro-*p*-nitrophenyl-$\alpha$-maltotrioside), the lactate dehydrogenase substrate (lactate), and the indicator for lactate dehydrogenase assay (nicotinamide adenine dinucleotide) were purchased from Sekisui Diagnostics Chemical Ltd (Exton, PA). Two-bis (2-aminophenoxy)-ethane-*N,N,N′,N′*-tetraacetic acid (BAPTA), the caspase-3, -7 substrate Z-DEVD-AMC (benzyloxycarbonyl-Asp-Glu-Val-Asp-7-amino-4-methylcoumarin), and the pancaspase substrate rhodamine 110 bis (l-aspartic acid amide) (D2R110) were obtained from Life Technologies (Carlsbad, CA). The pancaspase inhibitor benzyloxycarbonyl-Val-Ala-Asp (OMe) fluoromethylketone; (Z-VAD-fmk or ZVAD) and polyvinyldifluoride membranes were purchased from EMD Millipore (Billerica, MA). Ridaifen B, a tamoxifen analog that is a known inducer of apoptosis,[15] was purchased from Sigma-Aldrich (St. Louis, MO). The luciferase-based adenosine triphosphate (ATP) assay was obtained from Perkin Elmer. Antibodies against RIP3 were purchased from Cell Signaling (Beverly, MA) while antibodies against total MLKL and phosphorylated MLKL were from Abcam (Cambridge, MA). Antibodies against RIP1 were from ProSci (Poway, CA). Dulbecco's modified Eagle medium mixed 1:1 with Ham's F12 salts (DMEM-F12) and sodium pyruvate were from Life Technologies. Nitex mesh filters were purchased from Sefar America (Kansas City, MO). Necrostatin-1 was obtained from Enzo Life Sciences (Farmingdale, NY). Caerulein was purchased from Bachem (Torrance, CA). The TUNEL-staining kit was purchased from Millipore (Waltham, MA). For immunoprecipitation we used the Classic Magnetic IP/Co-IP kit from ThermoFisher Scientific (Waltham, MA). The enzyme-linked immunosorbent assays for monocyte chemoattractant protein 1 (MCP-1) and interleukin (IL)6 were purchased from R&D Systems, Minneapolis, MN). Taurolithocholic acid 3-sulfate disodium salt (TLCS), propidium iodide and all other chemicals were of analytic grade and purchased from Sigma-Aldrich (St. Louis, MO).

## Experimental Animals

All experiments were performed using non–sex-selected, wild-type C57Bl/6 mice (20–30 g) purchased from Jackson Labs (Bar Harbor, ME), or 20–30 g *RIP3*$^{-/-}$ mice, of either sex, that had been bred from founder C57Bl/6 knock-out animals kindly donated by Dr Xiaodong Wang (University of Texas Southwestern Medical Center).[16] These mice were back-crossed to a C57Bl/6 background for 10 generations. The animals were housed in temperature-controlled (23°C ± 2°C) rooms with a 12:12-hour light:dark cycle, fed standard laboratory chow, and allowed water ad libitum. All experiments were performed according to protocols approved by the Animal Care and Use Committee of the Tufts Medical Center.

## Preparation of Pancreatic Acini and Fragments

Pancreatic acini (1–100 cells per cluster) were freshly prepared for each experiment using collagenase digestion in

Dulbecco's modified Eagle medium (DMEM)-F12 as previously described.[17] They were suspended in DMEM/F12 containing 3 mmol/L Na-pyruvate and 0.01% (0.1 mg/mL) bovine serum albumin. The freshly prepared acini were passed through a 150-$\mu$m Nitex filter before use. For preparation of pancreatic fragments, freshly harvested portions of pancreas were minced, in the absence of collagenase, to create small ($<$0.5 mm$^3$) pieces as previously described.[18] In experiments involving BAPTA, Z-VAD-fmk, or necrostatin, the freshly prepared acini were incubated at 37°C for 30 minutes with or without BAPTA (20 $\mu$mol/L), Z-VAD-fmk (25 $\mu$mol/L), necrostatin (50 $\mu$mol/L), or vehicle (0.1% dimethyl sulfoxide [DMSO]) before incubation with TLCS or caerulein.

## Measurement of In Vitro Acinar Cell Necrosis

In vitro acinar cell injury/death was quantitated using 2 independent methods: (1) measuring the rate of lactate dehydrogenase (LDH) leakage from acini and (2) measuring the rate of propidium iodide (PI) uptake by acini. LDH activity was measured by determining the rate of increase in absorption at 340 nm resulting from the conversion of oxidized nicotinamide-adenine dinucleotide to reduced nicotinamide adenine dinucleotide when L-lactate is converted to pyruvate. By using the LDH technique, cell injury/death was quantitated by measuring the LDH activity in the acinar supernatant at the end of the incubation period (1, 2, 4, or 6 hours at 37°C) as a percentage of that noted after cell lysis with 0.5% Triton X-100 (Sigma-Aldrich, St. Louis, MO). For quantitation of cell injury/death using PI, the acini were plated in 96-well plates in medium containing 1 $\mu$g/mL PI. After incubation (1, 2, 4, or 6 hours at 37°C), PI fluorescence in the acini was quantitated with a Wallac-Victor fluorescence plate reader (Perkin Elmer, Waltham, MA) (excitation, 536 nm; emission, 617 nm). The acini then were lysed by addition of Triton X-100 (final concentration, 0.5%), and PI fluorescence was re-measured to determine the value of total PI fluorescence in the sample. When using the PI technique, cell injury/death was expressed as the percentage of total PI fluorescence that was observed after detergent lysis.

## Measurement of In Vitro Acinar Cell Apoptosis

The extent of acinar cell apoptosis was evaluated by quantitating TUNEL staining in pancreas fragments and by quantitating caspase activity in suspended acini. TUNEL staining was performed according to the kit manufacturer's instructions (Millipore, Waltham, MA) after incubation with test agents for 3 or 6 hours at room temperature. Caspase activity was measured as described previously.[19,20] Briefly, acini were harvested after predetermined periods of incubation with TLCS, caerulein, or ridaifen B. They were washed in microfuge tubes with Tris-buffered saline (TBS) by centrifugation at 300 $\times$ g for 60 seconds at room temperature and then homogenized and lysed in pH 7.5 buffer containing 50 mmol/L Tris HCl, 150 mmol/L NaCl, and 0.5 mmol/L EDTA. The samples were centrifuged at 15,000 $\times$ g for 15 minutes and the resulting supernatant then was incubated with 9 volumes of 25 mmol/L HEPES, pH 7.5, 10% sucrose, 0.1% 3-[(3-Cholamidopropyl)dimethylammonio]-1-propanesulfonate hydrate, 10 mmol/L dithiothreitol, and 20 $\mu$mol/L of the caspase-3, caspase-7 fluorogenic substrate Z-DEVD-AMC, or the caspase substrate D2R110. Fluorescence emission was measured at 440 nm after excitation at 360 nm (Z-DEVD-AMC), and at 521 nm after excitation at 498 nm (D2R110).

## Calculating the In Vitro Fractional Rate of Necroptotic Versus Apoptotic Acinar Cell Death

For these studies, we defined necroptotic cell death as the mode of cell death that could be inhibited by the RIP1 inhibitor necrostatin-1 and apoptotic cell death as the mode of cell death that could be inhibited by the pancaspase inhibitor ZVAD. Net TLCS-induced increases in PI uptake or LDH leakage were first calculated by subtracting the values obtained when acini were incubated with buffer alone (ie, PI uptake, 14.0% $\pm$ 2.0% of total; LDH leakage, 8.3% $\pm$ 2.5% of total) from the values obtained after acini were incubated with TLCS, TLCS + necrostatin, TLCS + ZVAD, TLCS + necrostatin + ZVAD. We believe that this subtraction is justified because it reflects the fact that suspensions of acini notoriously are contaminated by injured, dying, and dead cells that leak LDH and floating free nuclei that would be expected to bind PI. Those artifacts, created in the process of preparing suspensions of acini, would be expected to add to the noise of quantitating changes that really are indicative of events subsequently induced by test agents such as caerulein or TLCS, which, after all, was the purpose of our experiments. The same calculation was used to quantitate net caerulein-induced increases in PI uptake and LDH leakage. Once net caerulein- and TLCS-induced cell death had been calculated accurately, we expected that we would be able to quantitate more accurately the effects of necrostatin, ZVAD, or necrostatin + ZVAD on the net TLCS- and caerulein-induced cell death.

## Fractionation of Acinar Cells to Yield a Necrosome-Containing Pellet

After varying periods of incubation at 37°C with test agents, the acini were harvested by centrifugation (60 s, 300 $\times$ g) and then washed at 4°C with TBS containing a cocktail of protease inhibitors (Complete; Roche Diagnostics, Indianapolis, IN), 1 mmol/L phenylmethylsulfonyl fluoride, and phosphatase inhibitors (1 mmol/L NaF, 1 mmol/L $\beta$-glycerophosphate, and 1 mmol/L sodium orthovanadate). The cells then were lysed in the same buffer containing 1% NP-40 and the lysate was centrifuged (20,000 $\times$ g) for 15 minutes at 4°C.[7,8,10] The NP-40 soluble supernatant was substituted with one-quarter volume of 5$\times$ Laemmli buffer, and the NP-insoluble necrosome-containing pellet was dissolved in Laemmli buffer in volume equal to that of the supernatant and boiled for 2 minutes to achieve complete denaturation.

## Immunoblot Studies of the Necrosome-Containing Fractions

Proteins in the acinar cell fractions were separated by sodium dodecyl sulfate–polyacrylamide gel electrophoresis

10% and transferred to polyvinyldifluoride membranes. Empty sites were blocked with 0.1% bovine serum albumin in TBS containing 0.05% Tween-20. The membranes then were incubated overnight at 4°C with the primary antibody (anti-RIP1, anti-RIP3, total-MLKL, or phospho-MLKL) at 0.5 μg/mL in TBS containing 0.05% Tween-20, followed by incubation with a goat anti-mouse or goat anti-rabbit horseradish peroxidase antibody (2 μg/mL) for 2 hours at room temperature. Positive bands were visualized with FluorChem (ProteinSimple, Inc, San Jose, CA) using the Promega chemiluminescence kit (Madison, WI).

### Immunoprecipitation to Obtain a Necrosome-Containing Immunoprecipitant

Cells were lysed in radioimmunoprecipitation assay buffer (50 mmol/L Tris, HCl, pH 7.4, 150 mmol/L NaCl, 0.5% sodium deoxycholate, 0.1% sodium dodecyl sulfate, and 1% N-40) in the presence of protease and phosphatase inhibitors, and immunoprecipitation was performed according to the manufacturer's instructions (Classic Magnetic IP/Co-IP kit; ThermoFisher Scientific, Waltham, MA). Briefly, the cell lysate was centrifuged at 300*g* for 60 seconds to remove debris and the supernatant was incubated with 1 μg/mL anti-RIP1 antibodies overnight at 4°C. Twenty-five microliters of the protein A/G magnetobeads were added and the sample was incubated while rotating at 4°C for 2 hours. The beads were washed 3 times and bound proteins were eluted with 0.1 mol/L glycine, HCl pH 2.5. The eluent was neutralized and subjected to immunoblot analysis with antibodies against RIP1 and RIP3.

### ATP Measurement

ATP levels were determined by the luminescence ATP detection assay system purchased from Perkin Elmer. Briefly, acini were treated with caerulein or TLCS for a predetermined time, and lysed by addition of half volume (50 μL) of lysis buffer. After mixing for 5 minutes, another 50 μL of substrate buffer containing D-luciferin and luciferase was added. The generated light was measured using the Wallac-Victor luminescence plate reader (Perkin Elmer). ATP depletion was calculated by subtracting the ATP levels found on acini incubated with certain reagents from the ATP levels found in control untreated acini. ATP depletion is presented as a percentage of control untreated acini.

### Induction of Pancreatitis and Evaluation of Pancreatitis Severity

Bile acid–induced pancreatitis was elicited by retrograde pancreatic duct infusion of 50 μL of 10 mmol/L TLCS in phosphate-buffered saline at a rate of 5 μL/min as described previously by our group.[21] Secretagogue-induced pancreatitis was elicited by giving mice hourly intraperitoneal injections of caerulein (50 μg/kg body weight per injection) for 12 hours. Animals were killed by $CO_2$ asphyxiation 20 hours after the retrograde pancreatic duct infusion or 24 hours after the start of caerulein administration. Thirty minutes before the induction of pancreatitis, mice to be treated with necrostatin received an intraperitoneal injection of 100 μL per 20 g mouse of a solution containing 1.20 mg/mL necrostatin in phosphate-buffered saline containing 5% DMSO. The final dose of necrostatin delivered was 6 mg/kg. Thirty minutes before the induction of pancreatitis, mice treated with ZVAD received an intraperitoneal injection of 200 μL per 20 g mouse of phosphate-buffered saline containing 1.17 mg/mL ZVAD and 5% DMSO. The final dose of ZVAD was 11.7 mg/kg. Control mice received only the vehicle. Pancreatitis severity was evaluated at the time of death by quantitating hyperamylasemia, pancreatic edema (ie, pancreatic water content), pancreatic inflammation (ie, pancreatic myeloperoxidase activity), and acinar cell injury/necrosis as previously described.[22] Randomly selected regions of the pancreas were used for measurements involving the gland in the caerulein-induced model because that model is characterized by changes that are distributed diffusely within the gland. On the other hand, pancreatic measurements in the bile acid model were all made using portions of the pancreatic head because that model is characterized by changes that primarily, and most reproducibly, are localized to the pancreatic head. For this purpose, the mouse pancreatic head was defined as the portion of the gland that is located within 5 mm of the lesser duodenal curvature.

### Measurement of Plasma Cytokine Levels

Plasma MCP-1 and IL6 levels during caerulein- and TLCS-induced pancreatitis were measured by enzyme-linked immunosorbent assay, according to the manufacturer's instructions (R&D Systems, Minneapolis, MN).

### Data Analysis

All results were expressed as mean ± SD values. Graphs and tables report results obtained from at least 3 independent in vitro experiments each performed at least in duplicate or, for in vivo experiments, in 5 and usually more independently evaluated animals in each group. The significance of differences was evaluated using a 2-tailed Student *t* test for paired values and 1-way analysis of variance when multiple groups were being compared. Significant differences are marked by asterisks in all Figures and defined as those associated with a *P* value less than .05.

## Results

Our studies involved either exposure of acini or fragments to TLCS or caerulein under in vitro conditions or induction of either the secretagogue or the bile acid model of in vivo pancreatitis. PI uptake and LDH leakage from acinar cells were used to quantitate in vitro cell death and morphometric measurement of cell injury/death in the pancreas were used to quantitate in vivo cell death.

### Time Course of In Vivo and In Vitro Acinar Cell Death

As shown in Figure 1*A*, both caerulein and TLCS trigger accelerated in vitro PI uptake by acinar cells, which is first

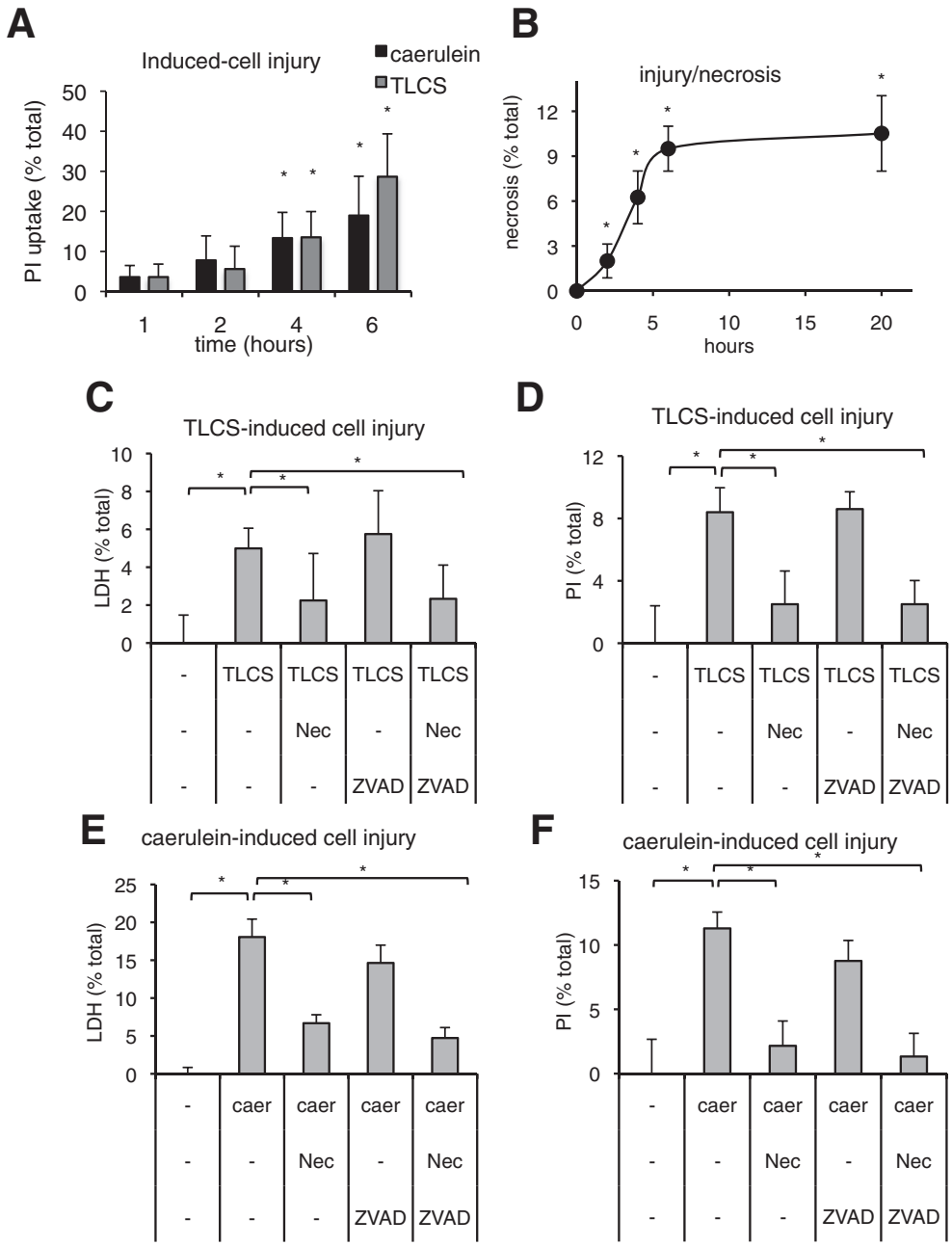


**Figure 1. Time dependence and mode of acinar cell injury/death after exposure to TLCS or caerulein.** (*A*) Time dependence of in vitro acinar cell injury/death after exposure to TLCS or caerulein. Acini were incubated with 250 $\mu$mol/L TLCS or 100 nmol/L caerulein for the indicated times and PI uptake was quantitated as described in the Materials and Methods section. *Asterisks* indicate a *P* value less than .05 when compared with untreated acini. (*B*) Time dependence of in vivo acinar cell injury/death after retrograde ductal infusion of TLCS. Mice were infused with TLCS to induce pancreatitis as described in the Materials and Methods section, and killed at the indicated times after completion of the infusion. Acinar cell injury/death was quantitated morphometrically and expressed as the percentage of acinar tissue. *Asterisks* indicate a *P* value less than .05 when compared with zero-time value. (*C–F*) In vitro cell death induced by TLCS or caerulein (caer) is inhibited by necrostatin-1 (nec), but not ZVAD. Acini were incubated for 4 hours in buffer containing 250 $\mu$mol/L TLCS or 100 nmol/L caerulein along with the RIP1 inhibitor necrostatin (50 $\mu$mol/L), the pancaspase inhibitor ZVAD (25 $\mu$mol/L), or necrostatin plus ZVAD. After incubation, net TLCS- and caerulein-induced PI uptake and LDH leakage over 4 hours were quantitated as described in the Materials and Methods section and expressed as a percentage of total PI uptake or LDH leakage measured after cell lysis with Triton X-100. The PI results show the average ± SD values of 5 experiments performed in quadruplicate and the LDH results are from 3 experiments performed in duplicate. *Asterisks* indicate a *P* value less than .05 when *bracketed columns* were compared.

**Table 1.** Percentage Reduction in TLCS-Induced Net Acinar Cell Injury/Death

| Conditions | PI uptake (% total) | *P* value | LDH leakage (% total) | *P* value |
|---|---|---|---|---|
| Necrostatin | 69.9 ± 16.5 | <.05 | 55.0 ± 14.6 | <.05 |
| ZVAD | −3.3 ± 0.8 | No reduction | -15.0 ± 14.6 | No reduction |
| Necrostatin + ZVAD | 69.4 ± 12.4 | <.05 | 53.2 ± 13.7 | <.05 |

NOTE. Freshly prepared pancreatic acini were incubated with 250 μmol/L TLCS for 4 hours in the presence of buffer alone, necrostatin, ZVAD, or necrostatin + ZVAD. PI uptake as well as LDH leakage were measured as described in the text and net PI uptake and LDH leakage were calculated by subtracting the values obtained with buffer alone. The percentage reduction in TLCS-induced net PI uptake and LDH leakage brought about by exposure to necrostatin, ZVAD, or necrostatin + ZVAD then was calculated. *P* values reflect the differences between the values obtained for PI uptake and LDH leakage triggered by TLCS alone.

statistically significant 4 hours after the start of incubation, and is even greater 6 hours after the start of incubation. As shown in Figure 1*B*, morphometric evidence of TLCS-induced in vivo cell injury/death is first apparent 2 hours after TLCS infusion, and further increases to reach a maximal level 6 hours after TLCS infusion.

## In Vitro Studies

*Necrotic cell death.* As shown in Figure 1*C–F*, incubation of acini with either 250 μmol/L TLCS or 100 nmol/L caerulein increases both PI uptake and LDH leakage. After incubation with 250 μmol/L TLCS alone for 4 hours the net increase in PI uptake was 8.4% ± 2.2% of total, whereas that for LDH leakage was 5.0% ± 1.4%. Similarly, after incubation with 100 nmol/L caerulein the net increase in PI uptake was 11.3% ± 2.3% of total, whereas that for LDH leakage was 18.1% ± 3.7%. These increases in net LDH leakage and PI uptake are reduced by pretreatment of the acinar cells with the necroptosis (and RIP1) inhibitor necrostatin, but increased net LDH leakage and PI uptake were not reduced by the apoptosis (and pancaspase) inhibitor ZVAD. Inclusion of both necrostatin and ZVAD results in net LDH leakage and PI uptake, which were the same as those noted when only necrostatin was added. More than 50% of the net cell death induced by TLCS or caerulein and quantitated by measuring either net LDH leakage or PI uptake was prevented by necrostatin, suggesting that it was the result of necroptosis, whereas virtually no reduction in either net TLCS- or caerulein-induced LDH leakage or PI uptake was elicited by ZVAD (Tables 1 and 2).

*Apoptotic cell death.* We used 2 separate but complementary techniques (TUNEL staining and caspase-3 and caspase-7 activation) to quantitate TLCS- or caerulein-induced apoptosis in pancreatic fragments. Ridaifen, which is a tamoxifen analog and a known inducer of apoptosis,[16,23] triggers extensive TUNEL staining of acinar cells (Figure 2*A* and *B*) and it increases caspase-3 and caspase-7 activity (Figure 2*C*). Both ridaifen-induced TUNEL staining and ridaifen-induced caspase activity are inhibited by ZVAD. We used ridaifen as an internal control to determine if pancreatic acini are capable of undergoing apoptosis, detected by TUNEL staining and caspase activation, under the conditions of our experiments. In contrast to ridaifen, however, neither caerulein nor TLCS trigger either TUNEL staining or an increase in caspase activity. In other apoptosis studies (not shown) performed using the caspase substrate D2R110, increased substrate cleavage initially presumed to reflect caspase activation was observed after exposure to ridaifen, TLCS, or caerulein, but that increased substrate cleavage was not inhibitable by the pancaspase inhibitor ZVAD, suggesting that it was not mediated by caspases but, more likely, by other, noncaspase acinar cell enzymes.

*Necrosome formation.* One of the initial events in the necroptotic mode of cell necrosis involves formation of a multimolecular scaffold-like complex known as the necrosome. For our studies of necrosome formation, 2 techniques were used. For most of our studies, acinar cells were lysed with detergent and, using centrifugation, 3 fractions were obtained: the total lysate; the high-speed

**Table 2.** Percentage Reduction in Caerulein-Induced Net Acinar Cell Injury/Death

| Conditions | PI uptake (% total) | *P* value | LDH leakage (% total) | *P* value |
|---|---|---|---|---|
| Necrostatin | 80.9 ± 3.2 | <.05 | 63.0 ± 8.9 | <.05 |
| ZVAD | 22.4 ± 0.8 | <.05 | 19.0 ± 5.5 | >.05 |
| Necrostatin + ZVAD | 88.2 ± 15.2 | <.05 | 73.9 ± 19.5 | <.05 |

NOTE. Freshly prepared pancreatic acini were incubated with 100 nmol/L caerulein for 4 hours in the presence of buffer alone, necrostatin, ZVAD, or necrostatin + ZVAD. PI uptake as well as LDH leakage were measured as described in the text and net PI uptake and LDH leakage were calculated by subtracting the values obtained with buffer alone. The percentage reduction in caerulein-induced net PI uptake and LDH leakage brought about by exposure to necrostatin, ZVAD, or necrostatin + ZVAD then was calculated. *P* values reflect the differences between the values obtained for PI uptake and LDH leakage triggered by caeruein alone.

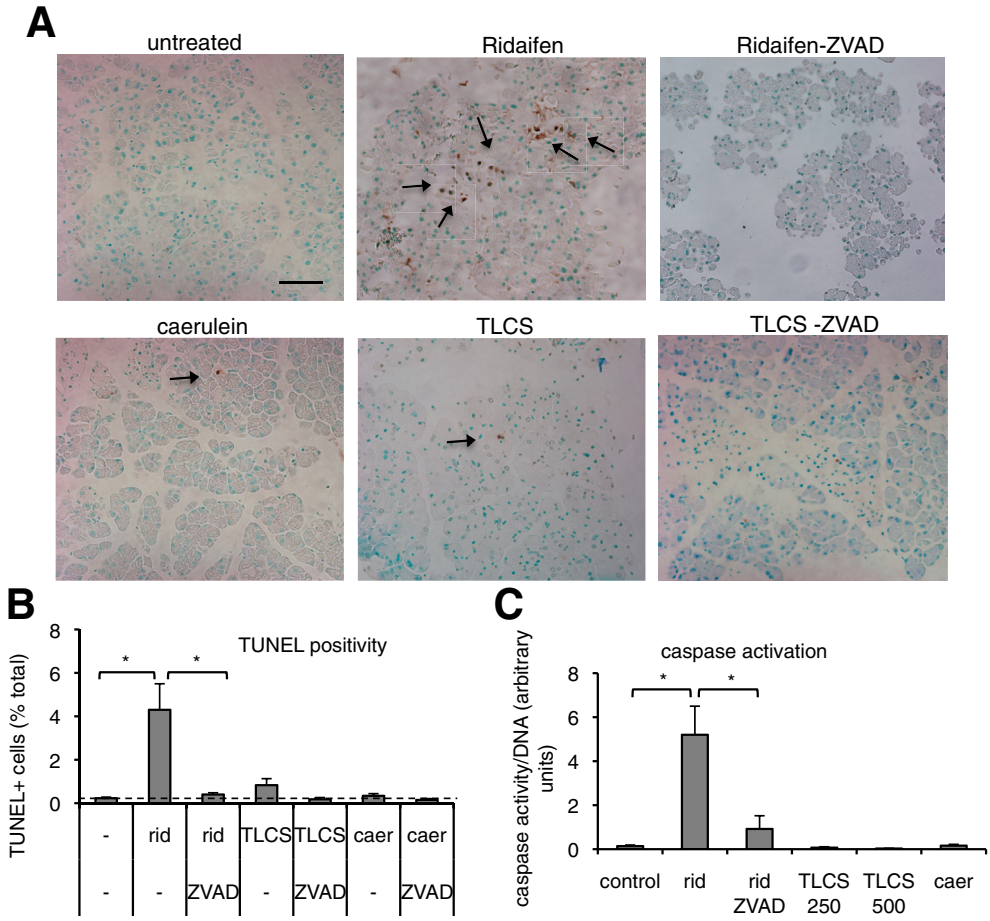


**Figure 2. Neither TLCS nor caerulein induce apoptotic acinar cell death.** (*A* and *B*) Ridaifen, but neither caerulein nor TLCS, triggers ZVAD-sensitive TUNEL positivity in acinar cells. Pancreas fragments were incubated with ridaifen (5 $\mu$mol/L), TLCS (250 $\mu$mol/L), or caerulein (100 nmol/L) with or without 25 $\mu$mol/L ZVAD for 3 hours. Sections were stained for TUNEL and counterstained with methyl green as described in the text. *Arrows* point to TUNEL-positive nuclei. (*A*) *Scale bar*: 50 $\mu$m. (*B*) *Columns* indicate means ± SD values from 2 experiments in which at least 5 fields (10×) containing more than 2000 cells were counted. *Horizontal dashed line* indicates control values for samples incubated with buffer alone. *Asterisks* denote a *P* value less than .05 when *bracketed columns* were compared. (*C*) Ridaifen (rid), but neither caerulein nor TLCS, triggers ZVAD-sensitive caspase activation. Freshly prepared acini were incubated with 250 $\mu$mol/L TLCS, 100 nmol/L caerulein, or 5 $\mu$mol/L ridaifen B for 2 hours and then washed with saline. They were lysed and caspase activity in the lysed samples was measured using the fluorogenic caspase substrate DEVD-AMC as described in the Materials and Methods section. *Columns* indicate means ± SD values from 3 experiments performed in duplicate. *Asterisks* indicate a *P* value less than .05 when *bracketed columns* were compared.

supernatant; and the high-speed, detergent-insoluble pellet. Others have used this technique and shown that necrosomes are located in this high-speed, detergent-insoluble fraction.[7,8] For confirmatory in vitro studies examining necrosome formation, we used a second technique: evaluation of RIP1/RIP3 co-immunoprecipitation from detergent-lysed acini. As shown in Figure 3*A* and *B*, exposure of acini to either caerulein or TLCS for 2 hours leads to formation of a detergent-insoluble pellet that contains both RIP1 and RIP3. As shown in Figure 3*C*, co-immunoprecipitation of RIP1 and RIP3 can be first detected in the lysate of cells exposed to either caerulein or TLCS for 2 hours.

As shown in Figure 3*D–G*, RIP1 and RIP3 are co-fractionated in the detergent-insoluble pellet of cells exposed to either caerulein or TLCS, and that co-fractionation is prevented by inclusion of necrostatin along with caerulein or TLCS in the incubation mixture. In addition to RIP1 and RIP3, MLKL also can be detected in the detergent-insoluble pellet obtained from cells incubated with either caerulein or TLCS (Figure 3*H* and *I*) and the total cell lysate contains phospho-MLKL (p-MLKL) in addition to total MLKL (Figure 3*J*). Finally, as shown in Figure 3*K* and *L*, co-fractionation of RIP1 in the detergent-insoluble pellet is not altered by inclusion of ZVAD along with caerulein or TLCS in the cell incubation mixture.

*Effects of RIP3 genetic deletion on TLCS- and caerulein-induced cell death and necrosome formation.* Enhanced LDH leakage, indicative of acinar cell death after exposure to either TLCS or caerulein, was reduced in cells obtained from *RIP3*$^{-/-}$ mice (Figure 4*A*) and

RIP1 was not detected in the detergent-insoluble fraction of *RIP3*$^{-/-}$ acinar cells exposed to either caerulein or TLCS (Figure 4*B*).

*ATP depletion.* Reports by other investigators have indicated that exposure of acinar cells to pancreatitis-inducing agents such as TLCS or caerulein can cause ATP depletion in acinar cells.[24,25] Our studies were designed to confirm these earlier findings and to determine if TLCS- or caerulein-induced ATP depletion leads to or is caused by necrosome formation and necroptosis. To accomplish this task, acinar cell ATP levels were monitored in cells incubated with either a prosecretory concentration of caerulein (10 pmol/L), a supramaximally stimulating concentration of caerulein (100 nmol/L), a low submicellar concentration of TLCS (100 $\mu$mol/L), or a cell death-inducing, submicellar concentration of TLCS (250 $\mu$mol/L). As shown in Figure 5*A* and *B*, statistically significant reductions in ATP levels were detected 60 minutes after acini are exposed to the higher concentrations of either TLCS or caerulein, but ATP depletion was not altered by inclusion of necrostatin in the incubation mixture (Figure 5*C*).

*Effects of calcium chelation on TLCS-induced ATP depletion and on acinar cell death induced by either caerulein or TLCS.* Accelerated calcium influx and pathologic increases of cytoplasmic calcium levels have been observed by us and others[26–29] to occur within seconds

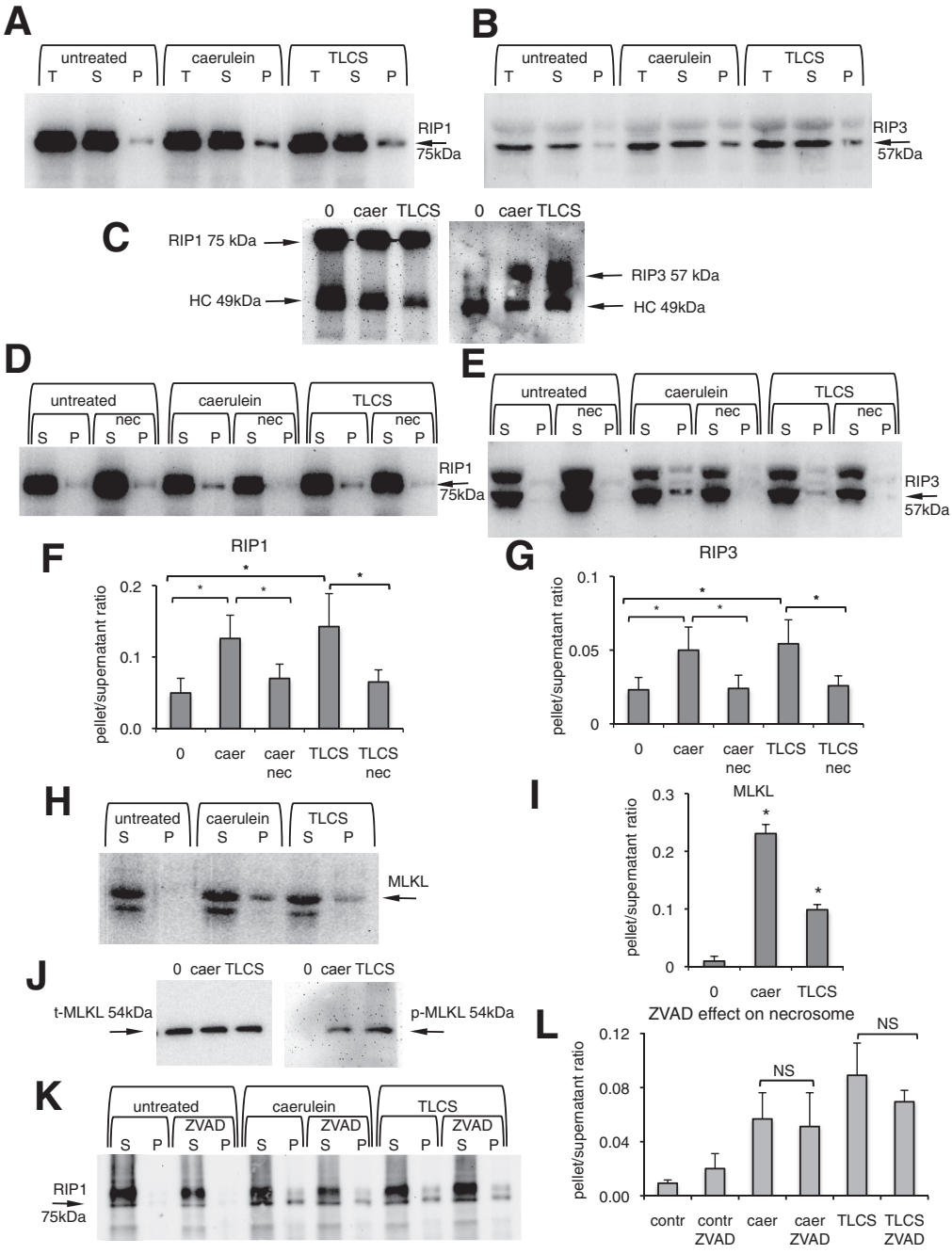

after exposing acinar cells to agents such as TLCS or caerulein, which trigger pancreatitis. Preloading acinar cells with the calcium chelator BAPTA can reduce or prevent those pathologic calcium increases or trypsinogen activation.[30] We show that preloading cells with BAPTA also prevents the following: (1) ATP depletion (Figure 6*A*), (2) necrosome formation (Figure 6*B* and *C*), and (3) accelerated PI uptake (Figure 6*D*) after exposure of acini to either caerulein or TLCS.

### In Vivo Studies

*Necrostatin-1 reduces the severity of either bile acid (TLCS)-induced or secretagogue (caerulein)-induced pancreatitis.* To examine TLCS-induced pancreatitis, mice were given an intraperitoneal dose of 6 mg/kg necrostatin with or without 11.7 mg/kg ZVAD 30 minutes before intraductal infusion of TLCS and then killed 20 hours after TLCS infusion. As shown in Figure 7*A*, the morphologic severity of pancreatitis was reduced in mice pretreated with necrostatin but not in mice pretreated with ZVAD, and the combination of necrostatin plus ZVAD resulted in the same severity observed when only necrostatin was given. The morphologic severity of TLCS-induced pancreatitis also was reduced in *RIP3*$^{-/-}$ mice (Figure 7*A*). When individual parameters of pancreatitis severity were quantitated separately, necrostatin and genetic deletion of RIP3, but not ZVAD, reduced the magnitude of pancreatic edema (ie, increased pancreas water content), neutrophil infiltration (ie, pancreas myeloperoxidase content), and morphometrically quantitated acinar cell injury/necrosis (Figure 7*B*–*D*). Plasma IL6 and MCP-1 levels also were increased 20 hours after intraductal infusion of TLCS, and that increase was reduced by administration of necrostatin or genetic deletion of *RIP3*. When secretagogue-induced pancreatitis was elicited, very similar results were obtained (Figure 8*A*–*D*, *F*, and *G*), however, in this case, pancreatic neutrophil infiltration (Figure 8*E*) was not altered by necrostatin, ZVAD, or *RIP3* deletion.

*Delayed administration of necrostatin after ductal infusion of TLCS.* As shown in Figures 7 and 8, in vivo acinar cell injury/death was reduced by administration of necrostatin 30 minutes before intraductal infusion of TLCS. We performed an additional series of studies designed to determine if the extent of in vivo acinar cell injury/death in TLCS-induced pancreatitis could also be reduced if necrostatin was administered hours after intraductal infusion of TLCS. As shown in Figure 9*A* and *B*, the morphologic severity and the morphometric extent of acinar cell injury/necrosis in TLCS-induced pancreatitis was reduced by administration of necrostatin even if it was given 2 or 4 hours after the completion of TLCS infusion. As shown in Figure 9*C*, acinar cell injury/necrosis in TLCS-induced pancreatitis was first observed 2 hours after TLCS infusion. It continued to increase until 6 hours after TLCS infusion when it reached a plateau level that remained constant until the time of death 20 hours after TLCS infusion. That continued increase in acinar cell injury/necrosis was not observed when mice were given necrostatin either 2 or 4 hours after TLCS infusion. The progression of TLCS-induced acinar cell injury/death was halted at the time of necrostatin administration and the extent of injury/necrosis observed at 20 hours remained essentially identical to that observed at the time of necrostatin administration.

## Discussion

The factors that determine the mode of acinar cell death during pancreatitis as well as its extent are poorly understood but it generally is believed that reducing acinar cell death during an attack of acute pancreatitis would effect its outcome favorably. Over the years, students of pancreatitis have identified a number of interventions that were found to reduce pancreatitis severity, however, for the most part,

**Figure 3.** (***See previous page***). **TLCS- and caerulein-induced in vitro acinar cell death is associated with necrosome formation.** (*A* and *B*) Effect of TLCS and caerulein on necrosome formation. Freshly prepared acini were incubated for 2 hours in buffer ± 250 μmol/L TLCS or 100 nmol/L caerulein (caer) ± necrostatin-1 (nec). After detergent lysis, samples containing the total lysate (T), the high-speed supernatant (S), and the high-speed, detergent-insoluble pellet (P) were obtained as described in the Materials and Methods section. These 3 fractions were subjected to immunoblot analysis using antibodies raised against RIP1 and RIP3. (*C*) Co-immunoprecipitation for RIP1 and RIP3. Samples were immunoprecipitated with anti-RIP1 antibodies and protein A/G magnetic beads as described in the Materials and Methods section. After elution from the beads the immunoprecipitants were subjected to immunoblot analysis with antibodies against RIP1 (*left*) and RIP3 (*right*) (HC points to IgG heavy chain). (*D*–*G*) Effect of necrostatin on necrosome formation. Acini were incubated with caerulein or TLCS ± necrostatin and then fractionated to yield a high-speed supernatant (S) and a high-speed, detergent-insoluble pellet (P). Those fractions then were immunoblotted using (*D*) anti-RIP1 antibodies or (*E*) anti-RIP3 antibodies. (*F* and *G*) Quantitation of immunoblots shown in panels *D* and *E*, respectively. The ratio of staining in the high-speed necrosome pellet to that in the high-speed supernatant is shown. *Bracketed columns* with *asterisks* denote differences with a *P* value less than .05. (*H* and *I*) Effect of caerulein and TLCS on transfer of MLKL to the necrosome. Samples were prepared and analyzed as described for panels *D*–*G*. *Asterisks* indicate a *P* value less than .05 when compared with samples not exposed to either TLCS or caerulein. (*I*) Quantitation of *blots* in panel *H* is shown. (*J*) Exposure of acini to caerulein or TLCS leads to MLKL phosphorylation. Acini were incubated for 2 hours with buffer, 100 nmol/L caerulein, or 250 μmol/L TLCS and lysed with detergent. The lysate was immunoblotted using anti-total MLKL (*left*) and anti–phospho-MLKL (*right*) antibodies. (*K* and *L*) Effect of ZVAD on TLCS or caerulein-induced necrosome formation. Samples were prepared and analyzed as described for panels *D*–*G*. *Asterisks* indicate a *P* value less than .05 when compared with samples not exposed to either TLCS or caerulein. (*K*) Shows immunoblot and (*L*) reports results of immunoblot quantitation. (*F*, *G*, *I*, and *J*) *Columns* indicate means ± SD values from 3 independent experiments. NS, statistically nonsignificant differences when *bracketed columns* were compared.

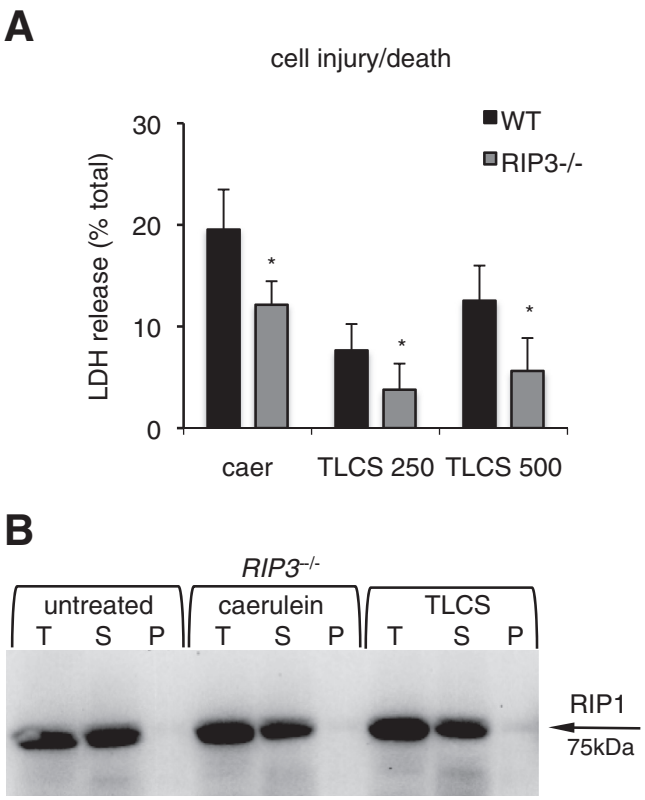


**Figure 4. Genetic deletion of RIP3 reduces LDH leakage and necrosome formation in acinar cells exposed to either TLCS or caerulein (caer).** (*A*) LDH leakage. Acini from wild-type and *RIP3*$^{-/-}$ mice were prepared and incubated with caerulein (100 nmol/L) or TLCS (250 or 500 $\mu$mol/L) for 4 hours. Cell injury was quantitated by measuring LDH leakage as described in the Materials and Methods section. *Columns* show the results of 3 independent experiments performed in duplicate. *Asterisks* denote a *P* value less than .05 when results from *RIP3*$^{-/-}$ mice are compared with wild-type animals. (*B*) Immunoblot. Acini from wild-type and *RIP3*$^{-/-}$ mice were incubated with TLCS or caerulein for 2 hours as described in the Materials and Methods section. Necrosome formation was evaluated using anti-RIP1 antibodies as shown in Figure 3*A*. The acini were lysed and fractions containing the total lysate (T), the high-speed supernatant (S), and the high-speed necrosome pellet (P) were isolated. They were subjected to immunoblot analysis using antibodies to RIP1. Note the absence of RIP1 staining in the necrosome fraction (P) of *RIP3*$^{-/-}$ cells exposed to either caerulein or TLCS compared with wild-type cells in Figure 3*A*.

those interventions have been found to be ineffective if instituted after the onset of the disease. Unfortunately, the vast majority of patients with severe pancreatitis only report to the hospital and become identified many hours or even days after the onset of pancreatitis and, for those patients, the identified potential interventions have not proven to be beneficial. As a result, no specific and effective therapy for acute pancreatitis has been identified and most patients remain dependent on nonspecific, symptomatic treatments. It generally is believed that the goal of developing effective treatments for severe pancreatitis will be met only if therapies that are effective even after the onset of severe pancreatitis can be identified.

Apoptotic and necroptotic cell death are the 2 most widely studied modes of regulated cell death and we considered both of these modes of cell death to be candidates for involvement in pancreatitis-associated cell death. Apoptotic cell death is usually a relatively benign, noninflammatory form of cell death in which cells and nuclei become pyknotic, cellular organelles fragment, and organelles as well as cells eventually are phagocytosed by neighboring cells or invading professional phagocytic cells. Most examples of apoptosis are caspase-dependent and inhibited by pancaspase inhibitors such as ZVAD. In contrast to apoptosis, necroptosis potentially is a much more aggressive mode of cell death. It is associated with plasma membrane rupture, extravasation of cytoplasm and intracellular elements, and an intense inflammatory response. Necroptotic cell death is believed to be initiated by activation of RIP1 kinase and formation of necrosomes. Small-molecule necrostatins, such as necrostatin-1, and genetic deletion of RIP3 prevent necroptosis by preventing RIP1 activation and inhibiting necrosome formation.

We performed both in vitro and in vivo experiments in efforts to achieve our 4 primary goals. The in vitro experiments involved suspending pancreatic acini or fragments in buffer containing either a supramaximally stimulating concentration of caerulein or a pancreatitis-inducing submicellar concentration of TLCS while in vivo experiments involved either repetitive hourly administration of a supramaximally stimulating dose of caerulein or retrograde pancreatic ductal infusion of TLCS.

We found that suspension of acini in TLCS- or caerulein-containing medium accelerated LDH leakage from the acini and enhanced PI uptake into the acini. These manifestations of cell death were first detectable 4 hours after acini were exposed to TLCS or caerulein and they increased further over the next 2 hours. We also found that intraductal infusion of TLCS, which elicits severe pancreatitis in mice, also caused extensive acinar cell injury/death that could be measured by morphometric quantitation of injured or dead acinar cells. It was first detectable 2 hours after the start of TLCS infusion, increased further over the next 4 hours, and then remained constant until the time of death 20 hours after the start of TLCS infusion.

To identify the mode of in vitro and in vivo acinar cell death, we added either necrostatin-1 or ZVAD to the in vitro incubation mixture containing either caerulein or TLCS and we pretreated mice with either necrostatin or ZVAD before either intraductal infusion of TLCS or dosing with caerulein. We found that, under in vitro conditions, necrostatin inhibited more than 50% of the cell death induced by either caerulein or TLCS while virtually none of that cell death was reduced by ZVAD, and the combination of necrostatin with ZVAD yielded results that were the same as those achieved with necrostatin alone. Similarly, we found that administration of necrostatin before the onset of TLCS infusion reduced acinar cell injury/death under in vivo conditions but no reduction in acinar cell injury/death was observed in mice given ZVAD. Together, these observations indicated that, under either in vitro or in vivo conditions, most (ie, >50%) of the acinar cell death observed in acini incubated

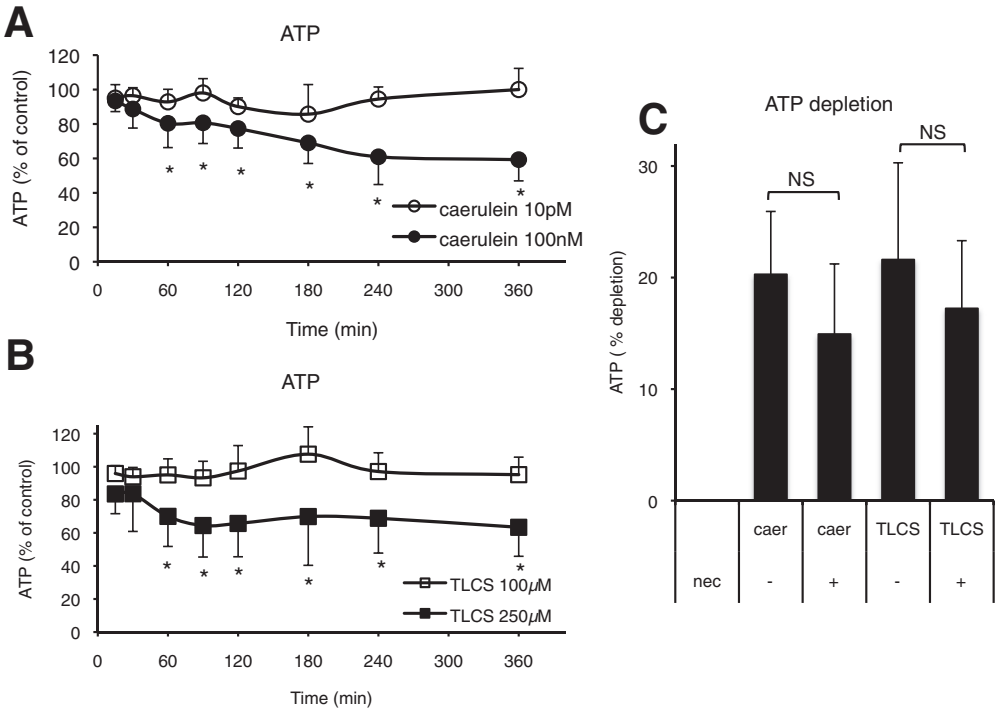


**Figure 5. Pancreatitis-inducing concentrations of caerulein or TLCS trigger acinar cell ATP depletion that is not prevented by necrostatin (nec).** (*A*) ATP depletion in response to 100 nmol/L caerulein (caer). Acini were suspended in buffer containing either a secretory concentration or a pancreatitis-inducing concentration of caerulein (ie, 10 pmol/L or 100 nmol/L, respectively) and ATP levels at the indicated times were quantitated as described in the Materials and Methods section. *Asterisks* indicate a *P* value less than .05 when ATP levels noted in samples exposed to 100 nmol/L caerulein were compared with control untreated acini. (*B*) ATP depletion in response to TLCS. Experiments were performed as described in panel *A*, but using either 100 μmol/L or 250 μmol/L TLCS. ATP levels at the indicated times were quantitated as described in the Materials and Methods section. The results are from 5 independent experiments performed in quadruplicate. *Asterisks* indicate a *P* value less than .05 when the ATP level noted in 250 μmol/L TLCS was compared with the ATP level noted in control untreated acini. (*C*) Necrostatin does not prevent caerulein or TLCS-induced ATP depletion. Acini were incubated with 100 nmol/L caerulein or 250 μmol/L TLCS ± 50 μmol/L necrostatin for 60 minutes and ATP levels were measured as described in the Materials and Methods section. *Columns* show the means ± SD from 5 independent experiments performed in quadruplicate. NS over *bracketed bars* indicates statistically nonsignificant differences in ATP levels.

with either caerulein or TLCS or in mice given injections of caerulein or ductal infusions of TLCS was necroptotic cell death and little or none of that cell death occurred by apoptosis. Studies directly measuring apoptosis in pancreas fragments by TUNEL staining or caspase activity supported that conclusion and they also showed that inhibition of necroptosis with necrostatin did not trigger a compensatory increase in apoptosis. Presumably, the TLCS and caerulein-induced acinar cell death that remained unaccounted for after administration of necrostatin and ZVAD (ie, 20%–40%) occurred by other nonapoptotic or non-necroptotic mechanisms.

The mechanisms of necroptosis have been studied extensively in other nonpancreatic tissues.[7,15,31] As a regulated form of programmed necrosis, it is defined by its dependence on early activation of RIP1 and by the fact that it is initiated by formation of necrosomes. We examined the process of necroptosis in acinar cells undergoing TLCS- or caerulein-induced in vitro cell death to determine if necrosome formation under those conditions conforms to the characteristics known to be typical of necroptosis in other cell types. We used 2 techniques to characterize necrosome assembly in our studies: the classic technique of immunoprecipitation in which 2 or more co-localized proteins are co-immunoprecipitated by antibodies directed at only one of the proteins; and an alternative technique that involves detergent lysis of cells followed by centrifugal fractionation and harvesting of a high-speed detergent-soluble supernatant and a high-speed detergent-insoluble pellet, the latter of which contains the assembling necrosomes.[7–9,28,30] In both techniques, proteins translocated to the assembling necrosomes were identified by immunoblot. For ease of presentation, these 2 techniques for studying necrosome assembly will be referred to as immunoprecipitation and fractionation.

By using either the fractionation technique or the immunoprecipitation technique, we found that both RIP1 and RIP3 translocate to the necrosome-containing fraction of acinar cells exposed to either caerulein or TLCS. In other studies performed using the fractionation technique, we found that RIP1 and RIP3 translocation can be prevented by necrostatin-1 but not by ZVAD. We also found that MLKL,

which is phosphorylated in cells exposed to caerulein or TLCS, also was translocated to the necrosome-containing fraction by exposure to caerulein or TLCS. Finally, we found that genetic deletion of RIP3 prevented acinar cell injury/death and it also prevented translocation of RIP1 to the necrosome fraction. Thus, each of these observations yielded the classic findings of necroptosis-related studies performed in other cell types and reported by many groups.[6,31–35] Many of those previously reported studies of necrosome formation used the immunoprecipitation technique. Our finding that identical results were observed using the fractionation technique supports the conclusion that the fractionation technique is a reliable method of studying necrosome formation. Our findings also strengthen our conclusion that TLCS and caerulein promote necroptotic cell death in pancreatic acinar cells and that conclusion is strengthened even further by our observation that, in both caerulein- and TLCS-induced pancreatitis, acinar cell injury/death can be prevented by administration of necrostatin-1.

It generally is believed that the earliest acinar cell changes during the evolution of caerulein- or TLCS-induced acute pancreatitis involve a sudden but transient and pathologic increase in cytoplasmic calcium levels and that aborting that increase by preloading cells with BAPTA can prevent subsequent downstream phenomena. We found that to be the case under in vitro conditions, that is, preloading acinar cells with BAPTA prevented caerulein and TLCS-induced ATP depletion, necrosome formation, and acinar cell injury/death. On the other hand, prevention of necroptosis by adding necrostatin to the caerulein or TLCS suspending medium does not interfere with TLCS- or caerulein-induced ATP depletion. Taken together, these observations aid in defining the sequence of events leading to acinar cell death in experimental caerulein- or TLCS-induced pancreatitis. They support the conclusion reached by other investigators[19,25,36–39] that caerulein- and TLCS-induced cell death follows, rather than precedes, depletion of acinar cell ATP levels and that ATP depletion, necrosome formation, and acinar cell injury/death all occur downstream of a pathologic increase in acinar cell cytoplasmic calcium levels.[30]

To pursue our third primary goal of determining if prevention of necroptosis would reduce the severity of experimental severe pancreatitis, we elicited caerulein- and TLCS-induced pancreatitis in wild-type and RIP3 knock-out mice and administered either necrostatin, ZVAD, or necrostatin plus ZVAD to the wild-type mice 30 minutes before the first dose of caerulein or 30 minutes before ductal infusion of TLCS. We found that the morphologic changes of both caerulein- and TLCS-induced pancreatitis,

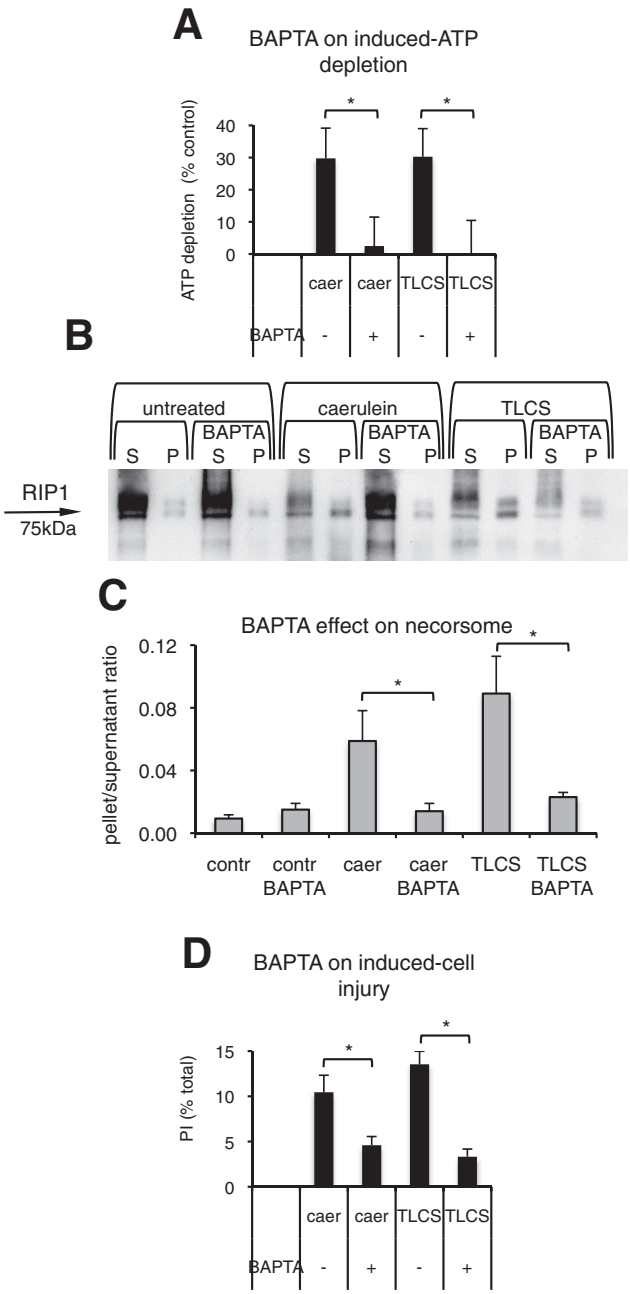


**Figure 6. Effect of intracellular calcium chelation on ATP depletion, necrosome formation, and on cell injury.** (*A*) BAPTA prevents caerulein (caer) and TLCS-induced ATP depletion. Acini were preincubated with or without BAPTA as described in the Materials and Methods section, and then exposed to 100 nmol/L caerulein or 250 $\mu$mol/L TLCS. ATP depletion was quantitated over 60 minutes as described in the Figure 5 legend. *Columns* show the means ± SD from 5 independent experiments performed in quadruplicate. *Asterisks* over *bracketed columns* indicate a *P* value less than .05. (*B* and *C*) BAPTA prevents caerulein and TLCS-induced necrosome formation. After preloading acini with or without BAPTA, necrosome formation was evaluated as described in Figure 3*A*. (*B*) Shows immunoblot and (*C*) reports results of immunoblot quantitation. *Columns* show the average ± SD from 3 independent experiments. (*D*) BAPTA prevents caerulein and TLCS-induced cell injury/death. Freshly prepared acini preloaded with or without BAPTA were exposed to caerulein (100 nmol/L) or TLCS (250 $\mu$mol/L) for 4 hours. PI uptake was quantitated as described in the Materials and Methods section and in Figure 1. *Columns* show the average ± SD from 5 independent experiments performed in quadruplicate. *Asterisks* indicate a *P* value less than .05 when *bracketed columns* were compared. Contr, control.

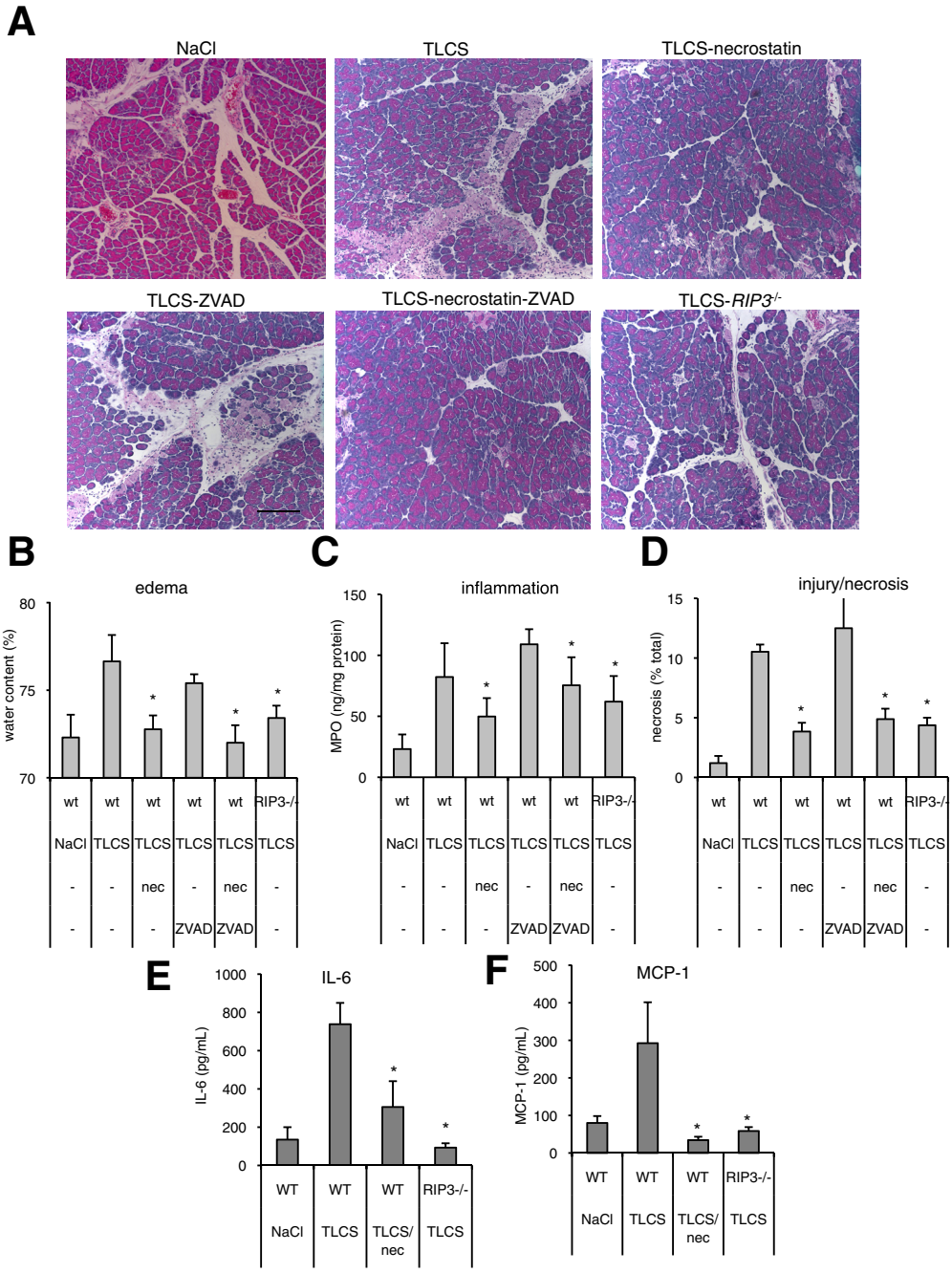


**Figure 7. Inhibition of RIP1 with necrostatin or genetic deletion of *RIP3* reduces the severity of TLCS-induced acute pancreatitis.** Acute pancreatitis was induced by retrograde pancreatic duct infusion of TLCS in wild-type (wt) and knockout (*RIP3*$^{-/-}$) mice as described in the Materials and Methods section, whereas control animals were infused only with saline. Randomly selected mice were pretreated with 6 mg/kg necrostatin (nec), 11.7 mg/kg ZVAD, or both. Mice were killed 20 hours after infusion. (*A*) Photomicrographs. Representative H&E-stained pancreas samples are shown. *Scale bar*: 200 $\mu$m. (*B–D*) Pancreatitis severity. Quantitation of edema, inflammation, and acinar cell injury/death was accomplished as described in the text. *Vertical columns* denote mean ± SD values from 5–9 mice in each group. *Asterisks* indicate statistically significant difference ($P < .05$) compared with wild-type mice with TLCS-induced pancreatitis that were not given necrostatin or ZVAD. (*E* and *F*) Necrostatin and genetic deletion of RIP3 reduce plasma IL6 and MCP-1 levels in TLCS-induced pancreatitis. Plasma samples were obtained at the time of death (20 hours after TLCS infusion), and MCP-1 as well as IL6 levels were measured as described in the Materials and Methods section.

as well as the individual parameters of pancreatitis severity (ie, edema, inflammation, injury) all were improved markedly by administration of necrostatin or by genetic deletion of RIP3, but no improvement was observed after administration of ZVAD. The improvement noted after the addition of both ZVAD and necrostatin was similar to that noted after

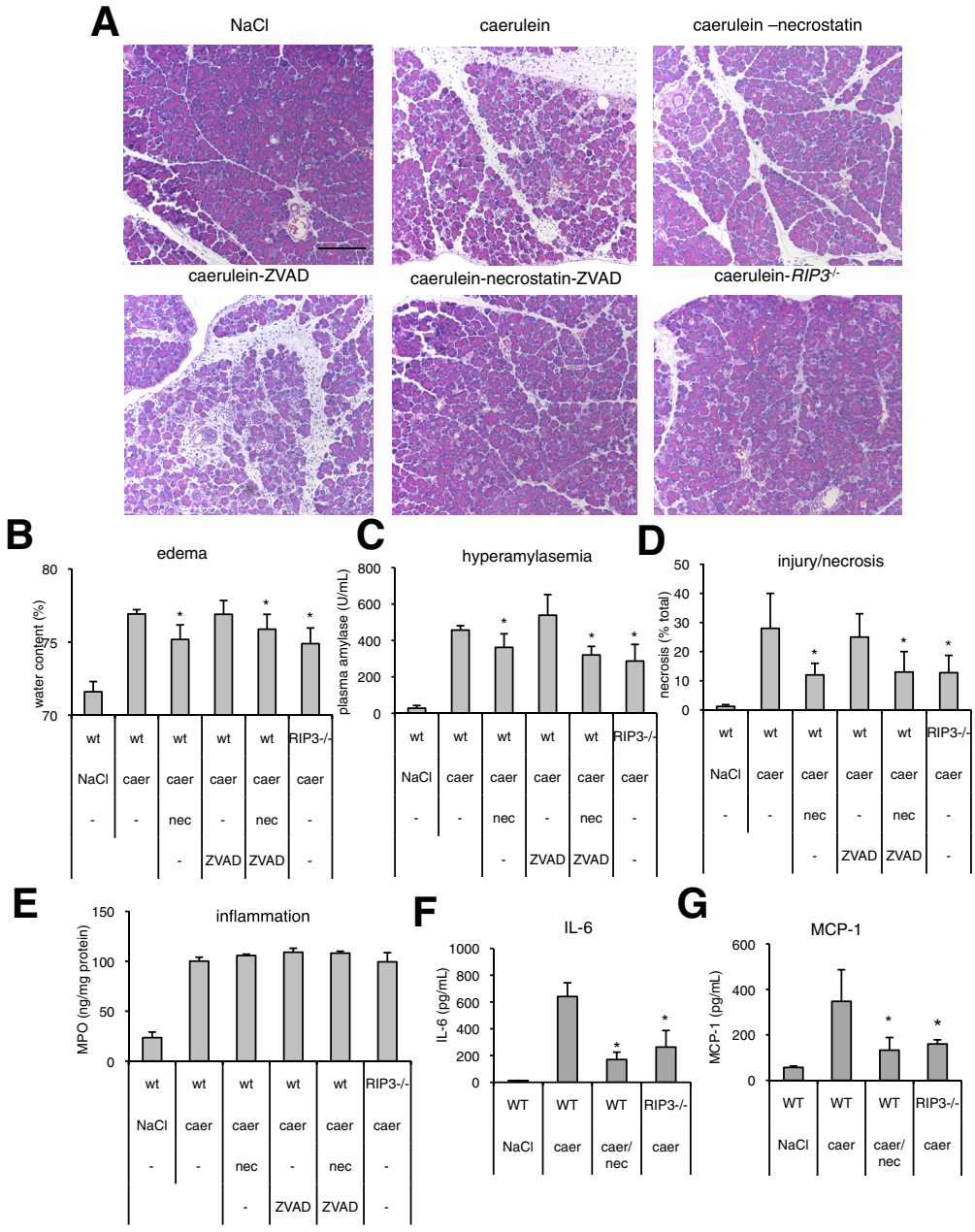


**Figure 8. Inhibition of RIP1 with necrostatin (nec) or genetic deletion of *RIP3* reduces the severity of caerulein-induced acute pancreatitis.** Caerulein-induced acute pancreatitis was elicited in wild-type (*RIP3*$^{+/+}$) and *RIP3*$^{-/-}$ mice by hourly intraperitoneal injections of caerulein (caer) (50 $\mu$g/kg/injection) given for 12 hours. Randomly selected mice were pretreated with 6 mg/kg necrostatin, 11.7 mg/kg ZVAD, or both. The animals were killed 24 hours after the start of caerulein administration. (*A*) Photomicrographs of H&E-stained samples of pancreas. *Scale bar*: 200 $\mu$m. (*B–E*) Pancreatitis severity. Pancreatitis severity was quantitated as described in Figure 7. *Columns* indicate mean ± SD values from 5 mice in each group. *Asterisks* indicate a *P* value less than .05 when compared with samples from wild-type mice that were not given necrostatin or ZVAD. (*F* and *G*) Necrostatin and genetic deletion of RIP3 reduce serum IL6 and MCP-1 levels in caerulein-induced pancreatitis. Plasma MCP-1 and IL6 levels were measured from blood obtained at the time of death. wt, wild-type.

addition of just necrostatin. The effects of necrostatin and RIP3 deletion on plasma chemocytokine levels at the time of death also were evaluated. We found that administration of necrostatin or genetic deletion of RIP3 markedly reduced IL6 and MCP-1 plasma levels in both models of severe pancreatitis. Taken together, these observations, made using in vivo mouse models of severe pancreatitis, indicate that the severity of those models can be reduced substantially by administration of necrostatin-1 or genetic deletion of RIP3, interventions that reduce the extent of necroptotic acinar cell death.

Several previously reported studies have examined the possibility that inhibition of necroptosis might protect against caerulein-induced pancreatitis.[14,40–42] Most studies have indicated that RIP3 deletion is protective, but 1 report indicated that necrostatin may increase caerulein-induced pancreatitis severity.[40] This discrepancy with our results may have to do with the necrostatin dose used. In that publication, the investigators administered 1.65 mg/kg necrostatin whereas we used 6 mg/kg. To our knowledge, there are no studies evaluating the effects of inhibiting necroptosis on the severity of bile acid–induced experimental pancreatitis. We were surprised to find that although all pancreatitis severity parameters (edema, acinar cell necrosis, systemic cytokine levels) in both models were reduced by necrostatin administration or *RIP3* deletion, pancreatic neutrophil infiltration was not reduced in the caerulein model of pancreatitis. Although histology indicates

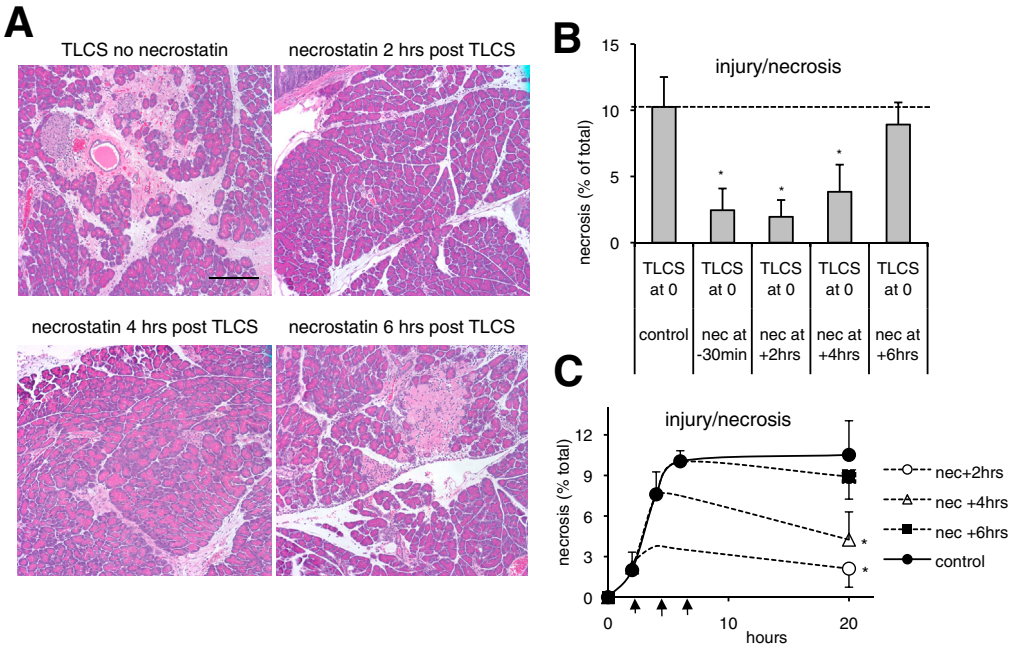


**Figure 9. Delayed administration of necrostatin (nec) halts progression of TLCS-induced acinar cell injury/necrosis.** (*A*) Representative photomicrographs are shown. Mice were infused with TLCS while necrostatin was administered at the indicated times before or after TLCS infusion. The mice were killed 20 hours after the start of TLCS infusion. *Scale bar*: 200 $\mu$m. (*B*) Time dependence of the necrostatin effect. Mice were infused with TLCS at zero time and given necrostatin at the indicated times either before or after TLCS infusion. They were killed 20 hours after TLCS infusion and TLCS-induced acinar cell injury/death was quantitated by morphometry. *Dashed line* defines extend of necrosis in control mice infused with TLCS at time 0 and never given necrostatin. (*C*) Necrostatin halts the progression of TLCS-induced acinar cell injury/death. Mice were infused with TLCS at zero time and killed 2, 4, or 6 hours later to quantitate TLCS-induced cell death at those times after TLCS infusion (*solid line*). Other mice infused with TLCS at zero time were given necrostatin at those times (2, 4, or 6 hours), but not killed at those times. Instead, they were killed 20 hours after TLCS infusion. *Columns* indicate mean ± SD values obtained from 5 mice in each group. *Asterisks* at 20 hours denote a *P* value less than .05 for those animals when compared with mice never given necrostatin. *Dashed line* allows for comparison of cell death immediately before necrostatin administration and cell death at the time of sacrifice.

that inflammatory cells were reduced, this appears not to be the case for neutrophils. We have no explanation for these discrepant findings.

Our fourth and final primary goal was to determine if inhibition of necroptotic cell death after the start of pancreatitis induction could reduce the extent of necroptotic cell death during TLCS-induced experimental pancreatitis. We chose to use the bile acid–induced model of pancreatitis for these studies because, in our opinion, its pathomechanism most closely resembles that of clinical acute biliary (gallstone) pancreatitis, which is the most common form of clinical acute pancreatitis. To test whether administration of necrostatin after the onset of pancreatitis could reduce acinar cell death in TLCS-induced pancreatitis, we changed our protocol for necrostatin administration. Rather than administer necrostatin 30 minutes before TLCS infusion, as we had performed in our earlier studies, we chose to administer necrostatin at selected times (2, 4, and 6 hours) after TLCS infusion. To evaluate the effects of this delayed administration of necrostatin, we would need to first determine the extent of acinar cell death present immediately before necrostatin administration (ie, 2, 4, or 6 hours after TLCS infusion) and then we would need to compare that value with the extent of acinar cell death that was present when necrostatin-treated mice were killed (ie, 20 hours after TLCS infusion).

Our findings were quite striking. We found that morphometrically quantitated acinar cell death in mice infused with TLCS but never given necrostatin was first increased roughly 2 hours after TLCS infusion and that it progressively became more increased over the ensuing 4 hours. It finally reached a plateau value 6 hours after TLCS infusion, and that plateau was maintained until the time of animal sacrifice 20 hours after TLCS infusion. The pattern of this response is explained most easily by concluding that TLCS infusion triggers progressive acinar cell injury/death for 6 hours but, thereafter, no additional acinar cell death occurs. Next, we administered necrostatin to TLCS-infused mice 2, 4, and 6 hours after TLCS infusion and quantitated acinar cell death at the time of sacrifice 20 hours after the TLCS infusion. We found that administration of necrostatin 2 or 4 hours after TLCS infusion had completely halted the progression of acinar cell death and the extent of acinar cell death at 20 hours was nearly identical to that observed immediately before necrostatin administration 2 or 4 hours after TLCS infusion. These findings indicate that administration of necrostatin completely halts the progression of acinar cell death in TLCS-induced pancreatitis and that the

final extent of cell death is determined by the extent of cell death that is present at the time of necrostatin administration. As a result, significant decreases in acinar cell death at 20 hours are achievable by administration of necrostatin 2 or 4 hours after TLCS infusion. Administration of necrostatin 6 hours after TLCS infusion fails to improve the extent of cell death at 20 hours, presumably because that process already has reached its maximal level at the time of necrostatin administration.

In summary, the studies reported in this article indicate the following: (1) necroptosis is the most prevalent mode of TLCS- and caerulein-induced in vitro cell death; (2) under in vitro conditions, TLCS- and caerulein-induced acinar cell necroptosis is characterized by necrosome formation and inhibitable by necrostatin administration or RIP3 deletion; (3) under in vitro conditions, TLCS- and caerulein-induced acinar cell necroptosis is dependent on a preceding pathologic increase in cytoplasmic calcium levels and it occurs after acinar cell ATP depletion; (4) the severity of both TLCS- and caerulein-induced pancreatitis is reduced by prior inhibition of necroptosis brought about by either necrostatin administration or RIP3 deletion; and (5) necrostatin can reduce acinar cell injury/death during TLCS-induced pancreatitis even if that necrostatin is administered after infusion of TLCS already has triggered the onset of experimental pancreatitis.

These observations, which come from mouse models of pancreatitis, do not guarantee that the same observations would be obtained in human pancreatitis or even in other rodent models. However, they suggest that inhibition of necroptosis might protect against clinical severe pancreatitis even if necroptosis inhibition is achieved after the onset of pancreatitis. In our experiments, necrostatin-1 was used to inhibit necroptosis but, in the case of clinical pancreatitis, other methods of inhibiting necroptosis, with differing pharmacodynamics and toxicities, might prove even more effective. The time course for clinical pancreatitis will need to be characterized carefully. Although we have shown that TLCS-induced pancreatitis in mice evolves over a 6-hour period and that the window for protection is open for roughly 4 hours, different times might be critical in clinical pancreatitis. Regardless of these considerations, however, our observations indicate that therapies designed to interfere with necroptosis might be an effective strategy for the treatment of severe clinical pancreatitis, which already has been established at the time of its diagnosis.

## References


1. Frossard JL, Steer ML, Pastor CM. Acute pancreatitis. Lancet 2008;371:143–152.
2. Yadav D, Lowenfels AB. The epidemiology of pancreatitis and pancreatic cancer. Gastroenterology 2013; 144:1252–1261.
3. Galluzzi L, Vitale I, Abrams JM, et al. Molecular definitions of cell death subroutines: recommendations of the Nomenclature Committee on Cell Death 2012. Cell Death Differ 2012;19:107–120.
4. Davidovich P, Kearney CJ, Martin SJ. Inflammatory outcomes of apoptosis, necrosis and necroptosis. Biol Chem 2014;395:1163–1171.
5. Holler N, Zaru R, Micheau O, et al. Fas triggers an alternative, caspase-8-independent cell death pathway using the kinase RIP as effector molecule. Nat Immunol 2000;1:489–495.
6. Li J, McQuade T, Siemer AB, et al. The RIP1/RIP3 necrosome forms a functional amyloid signaling complex required for programmed necrosis. Cell 2012;150: 339–350.
7. Sun L, Wang H, Wang Z, et al. Mixed lineage kinase domain-like protein mediates necrosis signaling downstream of RIP3 kinase. Cell 2011;148:213–227.
8. Moquin DM, McQuade T, Chan FK. CYLD deubiquitinates RIP1 in the TNFalpha-induced necrosome to facilitate kinase activation and programmed necrosis. PLoS One 2013;8:e76841.
9. Wu XN, Yang ZH, Wang XK, et al. Distinct roles of RIP1-RIP3 hetero- and RIP3-RIP3 homo-interaction in mediating necroptosis. Cell Death Differ 2014;21:1709–1720.
10. Bonapace L, Bornhauser BC, Schmitz M, et al. Induction of autophagy-dependent necroptosis is required for childhood acute lymphoblastic leukemia cells to overcome glucocorticoid resistance. J Clin Invest 2010; 120:1310–1323.
11. Kroemer G, Galluzzi L, Vandenabeele P, et al. Classification of cell death: recommendations of the Nomenclature Committee on Cell Death 2009. Cell Death Differ 2009;16:3–11.
12. Degterev A, Huang Z, Boyce M, et al. Chemical inhibitor of nonapoptotic cell death with therapeutic potential for ischemic brain injury. Nat Chem Biol 2005;1:112–119.
13. Degterev A, Yuan J. Expansion and evolution of cell death programmes. Nat Rev Mol Cell Biol 2008; 9:378–390.
14. Quarato G, Guy CS, Grace CR, et al. Sequential engagement of distinct MLKL phosphatidylinositol-binding sites executes necroptosis. Mol Cell 2016; 61:589–601.
15. Nagahara Y, Shiina I, Nakata K, et al. Induction of mitochondria-involved apoptosis in estrogen receptor-negative cells by a novel tamoxifen derivative, ridaifen-B. Cancer Sci 2008;99:608–614.
16. He S, Wang L, Miao L, et al. Receptor interacting protein kinase-3 determines cellular necrotic response to TNF-alpha. Cell 2009;137:1100–1111.
17. Sharma A, Tao X, Gopal A, et al. Calcium dependence of proteinase-activated receptor 2 and cholecystokinin-mediated amylase secretion from pancreatic acini. Am J Physiol Gastrointest Liver Physiol 2005;289:G686–G695.
18. Van Acker GJ, Perides G, Weiss ER, et al. Tumor progression locus-2 is a critical regulator of pancreatic and lung inflammation during acute pancreatitis. J Biol Chem 2007;282:22140–22149.
19. Gukovskaya AS, Gukovsky I, Jung Y, et al. Cholecystokinin induces caspase activation and mitochondrial dysfunction in pancreatic acinar cells. Roles in cell injury processes of pancreatitis. J Biol Chem 2002; 277:22595–22604.
20. Mareninova OA, Sung KF, Hong P, et al. Cell death in pancreatitis: caspases protect from necrotizing pancreatitis. J Biol Chem 2006;281:3370–3381.

21. Laukkarinen JM, van Acker GJ, Weiss E, et al. A mouse model of acute biliary pancreatitis induced by retrograde pancreatic duct infusion of Na-taurocholate. Gut 2007; 56:1590–1598.
22. Sharma A, Tao X, Gopal A, et al. Protection against acute pancreatitis by activation of protease-activated receptor-2. Am J Physiol Gastrointest Liver Physiol 2005;288:G388–G395.
23. Tsukuda S, Kusayanagi T, Umeda E, et al. Ridaifen B, a tamoxifen derivative, directly binds to Grb10 interacting GYF protein 2. Bioorg Med Chem 2013;21:311–320.
24. Liu Y, Yuan J, Tan T, et al. Genetic inhibition of protein kinase Cε attenuates necrosis in experimental pancreatitis. Am J Physiol Gastrointest Liver Physiol 2014; 307:G550–G563.
25. Mukherjee R, Mareninova OA, Odinokova IV, et al. Mechanism of mitochondrial permeability transition pore induction and damage in the pancreas: inhibition prevents acute pancreatitis by protecting production of ATP. Gut 2016, Epub ahead of print.
26. Dawra RK, Saluja AK, Runzi M, et al. Inositol trisphosphate-independent agonist-stimulated calcium influx in rat pancreatic acinar cells. J Biol Chem 1993; 268:20237–20242.
27. Voronina S, Longbottom R, Sutton R, et al. Bile acids induce calcium signals in mouse pancreatic acinar cells: implications for bile-induced pancreatic pathology. J Physiol 2002;540:49–55.
28. Booth DM, Murphy JA, Mukherjee R, et al. Reactive oxygen species induced by bile acid induce apoptosis and protect against necrosis in pancreatic acinar cells. Gastroenterology 2011;140:2116–2125.
29. Perides G, Laukkarinen JM, Vassileva G, et al. Biliary acute pancreatitis in mice is mediated by the G-protein-coupled cell surface bile acid receptor Gpbar1. Gastroenterology 2010;138:715–725.
30. Raraty M, Ward J, Erdemli G, et al. Calcium-dependent enzyme activation and vacuole formation in the apical granular region of pancreatic acinar cells. Proc Natl Acad Sci U S A 2000;97:13126–13131.
31. Silke J, Rickard JA, Gerlic M. The diverse role of RIP kinases in necroptosis and inflammation. Nat Immunol 2015;16:689–697.
32. Dondelinger Y, Declercq W, Montessuit S, et al. MLKL compromises plasma membrane integrity by binding to phosphatidylinositol phosphates. Cell Rep 2014; 7:971–981.
33. Wang X, Li Y, Liu S, et al. Direct activation of RIP3/MLKL-dependent necrosis by herpes simplex virus 1 (HSV-1) protein ICP6 triggers host antiviral defense. Proc Natl Acad Sci U S A 2014;111:15438–15443.
34. Zhao J, Jitkaew S, Cai Z, et al. Mixed lineage kinase domain-like is a key receptor interacting protein 3 downstream component of TNF-induced necrosis. Proc Natl Acad Sci U S A 2012;109:5322–5327.
35. Sun X, Yin J, Starovasnik MA, et al. Identification of a novel homotypic interaction motif required for the phosphorylation of receptor-interacting protein (RIP) by RIP3. J Biol Chem 2002;277:9505–9511.
36. Booth DM, Mukherjee R, Sutton R, et al. Calcium and reactive oxygen species in acute pancreatitis: friend or foe? Antioxid Redox Signal 2011;15:2683–2698.
37. Criddle DN, Gerasimenko JV, Baumgartner HK, et al. Calcium signalling and pancreatic cell death: apoptosis or necrosis? Cell Death Differ 2007;14:1285–1294.
38. Mukherjee R, Criddle DN, Gukovskaya A, et al. Mitochondrial injury in pancreatitis. Cell Calcium 2008;44:14–23.
39. Shalbueva N, Mareninova OA, Gerloff A, et al. Effects of oxidative alcohol metabolism on the mitochondrial permeability transition pore and necrosis in a mouse model of alcoholic pancreatitis. Gastroenterology 2013; 144:437–446 e6.
40. Linkermann A, Brasen JH, De Zen F, et al. Dichotomy between RIP1- and RIP3-mediated necroptosis in tumor necrosis factor-alpha-induced shock. Mol Med 2012; 18:577–586.
41. Ma X, Conklin DJ, Li F, et al. The oncogenic microRNA miR-21 promotes regulated necrosis in mice. Nat Commun 2015;6:7151.
42. Wu J, Huang Z, Ren J, et al. Mlkl knockout mice demonstrate the indispensable role of Mlkl in necroptosis. Cell Res 2013;23:994–1006.

**Received October 12, 2015. Accepted April 10, 2016.**

**Correspondence**
Address correspondence to: George Perides, PhD, Department of Surgery, Tufts Medical Center #37, 800 Washington Street, Boston, Massachusetts 02111. e-mail: peridesgeorge@gmail.com; fax: (617) 636-1466.

**Acknowledgments**
The authors are grateful to Dr Degterev for helpful discussions and advice on the use of necrostatin, Dr Mareninova for advice regarding the caspase activation experiments, and Dr Xiaodong Wang for the *RIP3*$^{-/-}$ mice.

**Conflicts of interest**
The authors disclose no conflicts.

**Funding**
This study was supported by the National Institutes of Health National Institute of Diabetes and Digestive and Kidney Diseases R01-091327 (M.L.S.) and the Sigrid Jusélius Foundation, Finland (J.L.).